JOURNAL OF OPTOELECTRONICS AND ADVANCED MATERIALS Vol. 12, No. 3, March 2010, p. 754 - 757

Physical and photocatalytic properties of laser fabricated crystalline TiO_2 at low temperatures

J. REMSA[a*], M. JELÍNEK[a,b], T. KOCOUREK[a,b], J. MIKŠOVSKÝ[b], V. STUDNIČKA[a], V. VORLÍČEK[a], V. SVÁTA[c], V. VYMĚTALOVÁ[a]
[a]*Institute of Physics ASCR, Na Slovance 2, 182 21 Prague 8, Czech Republic*
[b]*Czech Technical University in Prague, Faculty of Biomedical Engineering, nam. Sitná 3105, 272 01 Kladno , Czech Republic*
[c]*Institute of Physical chemistry ASCR, Dolejškova 2155/3, 182 23 Prague 8, Czech Republic*

We report on an extensive study of the deposition of titanium dioxide layers by pulsed laser deposition at either room temperature or at 200°C (300°C, 400°C, 500°C) from pure titanium and titanium dioxide targets. Some amorphous samples were annealed by the rapid thermal annealing method. The study is focused on the effect of variation of pressure of the reactive oxygen and the inert argon atmospheres, and the mixtures of both. The laser fluency varied in the range 2 J/cm^2 to 9 J/cm^2. The crystalline structure was characterized by X-ray diffraction and Raman Spectroscopy and for the study of the surface properties, atomic force microscopy was used. The TiO_2 photocatalytic characteristics were determined using 4-chlorphenol solution degradation evaluated by pH measurement. Polycrystalline (anatase, rutile, and brookite) and amorphous layers exhibiting photocatalytic behavior were obtained at low substrate temperatures (200°C).

(Received June 18, 2009; accepted December 15, 2009)

Keywords: Pulsed laser deposition, TiO_2, Contact angle, Photocatalytic properties, Thin films

1. Introduction

Titanium dioxide (TiO_2) is a commonly known semiconductor, especially known for its high refractive index, which is around 2.7 (at 500 nm) depending on the crystalline structure. It enables the use of TiO_2 in optical elements [1], e.g. anti-reflective coating. Other applications are microelectronics (varistors, field effect transistors, gas sensors), photocatalytic and antibacterial devices, and photovoltaic cells [2-6]. Such photocatalytic and antibacterial devices, for example for a new type of urinal catheter, are the motivation behind the work published in this paper. In most cases, these applications usually require crystalline TiO_2 in thin layer form.

To prepare TiO_2 layers, various methods such as electron-beam deposition, ion-assisted deposition, ion beam sputter deposition, activated reactive evaporation, ion plating, plasma plating, radio-frequency (RF) diode sputtering, dip coating, sol-gel, spin coating, anodization, oxygen plasma assisted molecular beam epitaxy, spray coating, and pulsed laser deposition (PLD) were implemented [1-7]. Also TiO_2 doping with nitrogen and sulfur [8], and composites synthesis, such as titania/hydroxyapatite [7] and ZnO/TiO_2 nanotubes [9], were published.

Creation of crystalline TiO_2 layers by the PLD method at low temperatures was reported in a limited number of experiment [3, 4, 5, 10, 11], but usually it is claimed that to obtain crystalline TiO_2 a substrate temperature of around 400°C is required [1].

TiO_2 occurs in nature as the well-known minerals rutile, anatase and brookite. Anatase and brookite both convert to rutile, which is an equilibrium crystalline phase, upon heating. Beside the change in the refractive index, the crystalline phase influences the mass density, the gap energy [12] and the electron-hole pair lifetime, which causes different photocatalytic activity [13].

In this contribution, we report the PLD of polycrystalline TiO_2 layers at low temperatures and the results of measurement photocatalytic properties for future medical application in the development of a urethral catheter.

2. Experimental

2.1 Deposition

The TiO_2 layers were grown using PLD with the Compex Pro 205 F KrF* excimer laser (λ= 248 nm, τ_{FWHM} = 20 ns, repetition rate 1-50 Hz), a stainless steel vacuum chamber and a target holder with resistive heating. The vacuum system consists of a turbomolecular pump following rotary and Roots pumps. The configuration enables to change the pressure continuously. The laser beam was focused by a fused silica lens (f = 250 mm) on the target, which was a disc with the diameter of 50 mm and thickness of 5 mm made from titanium (99.95%) or rutile (99.99%, pressed pellets). Silicon wafers (111) and fused silica, both with dimensions of 10×10 mm^2, were used as substrates. The chamber was evacuated to 10^{-3} Pa before the deposition, and then filled with either oxygen or argon or a mixture of both. Some samples were prepared at vacuum conditions.

The deposition oxygen pressure was varied from 0.1 Pa to 100 Pa, the argon from 266 Pa to 500 Pa, and in the case of O_2-Ar mixture the pressure moved from 1 Pa to 40 Pa. Different gas ratios were applied when using the mixture. The number of laser pulses was varied from 2,000 to 15,000. The laser fluencies ranged from 2 J/cm^2 to 9 J/cm^2 (laser spot from 1.4×2.4 mm^2 to 2.3×3.5 mm^2). The target–substrate distance (d_{ts}) was set to 40 mm. The substrate temperature (T_S) was maintained either at room temperature (RT) or at 200°C. Some layers were fabricated at 300°C, 400°C and 500°C. More information on deposition conditions can be found in Fig. 1 (deposition from pure titanium target) and in Fig. 2 (deposition from rutile target). The references in brackets in Fig. 2 show earlier published data of TiO_2 deposition at room T_S.

Rapid thermal annealing (JIPelec Jetfirst 100 Rapid Thermal Processor - RTA) is the process of fast heating of layers by halogen lamps. For RTA, we prepared 4 amorphous TiO_2 samples (rutile target, 4 J/cm^2, 3 Pa O_2). Three or five pulses (3 s or 6 s long) with 5 minutes break between the pulses were applied.

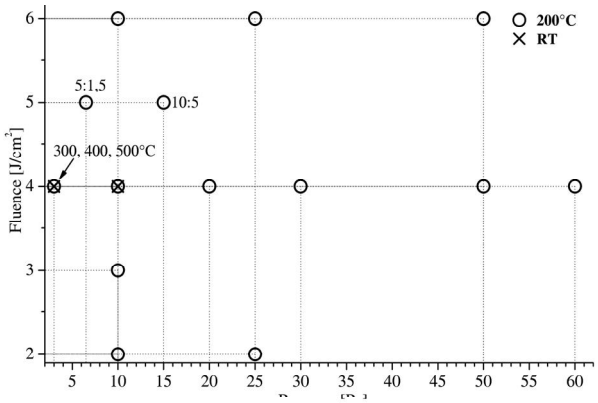

Fig. 1. The chart of deposition conditions for the titanium target. All layers were created at RT (×) or 200°C (O), in oxygen ambient, except those where stated otherwise [(O_2:Ar ratio, higher T_S (marked by arrow)].

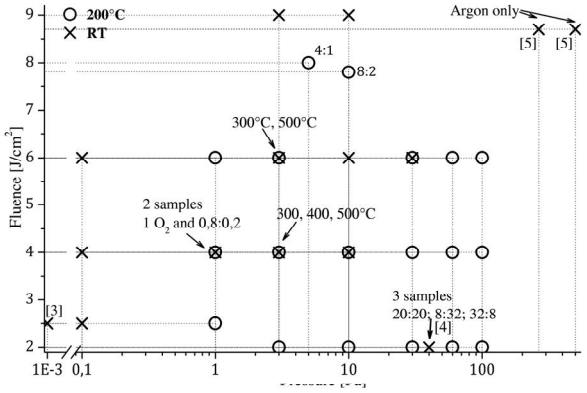

Fig. 2. The chart of deposition conditions for the rutile target. All layers were created at RT (×) or 200°C (O), in oxygen ambient, except those where stated otherwise [(O_2:Ar ratio, higher T_S (marked by arrow)].

2.2 Characterization

The layer thickness was determined by profilometric measurement (Alfastep IQ). For characterizing layer topography, the AFM type Solver NEXT (NT-MDT) in non-contact regime with NSG 11 tips was used.

The crystalline properties were measured by X-Ray diffraction (XRD) and Raman spectroscopy (RS). Parallel beam geometry, detector scan with the stationary sample, and the glazing angle of incidence (GAOI) were used for XRD. The GAOI, in our case five degrees, enables the whole sample illumination. Due to the GAOI method, the substrate spectrum is not present and for a polycrystalline material the peaks positions are the same as for a symmetric scan. The diffractometer was powered by a rotating anode generator X-ray source (300 mA, 55 kV). The RS setup consisted of Renishaw 1000 and inVia Reflex microscopes. Sample excitation was done at room temperature and at three different wavelengths using Argon (488 or 514.5 nm) or He-Ne laser (633 nm). The polarization was not analyzed.

The photocatalytic properties were determined by 4-chlorine phenol (4ClP) solution (3×10^{-3} mol) degradation. This method has been adapted according to [14, 15]. Each sample was put into a Suprasil cell (3.5 ml volume) with magnetic stirring and were continuously illuminated by a mercury flash lamp (8.75 mW/cm^2). To prevent the decomposition of molecules by UV irradiation alone, filtering wavelengths shorter than 360 nm were implemented. Additionally, an IR filter was used to prevent the cell heating. The cell temperature was lower than 30°C. The illuminated area was roughly 70 mm^2 and the sample plane was set to be perpendicular to the light source. The pH decrease over time expresses the sample photocatalytic properties. For the calculation of final pH change, the pH value from the 100th minute was taken and subtracted from the value from the 20th minute after the irradiation started.

3. Results and discussion

Firstly, we started with the repeating of published experiments, in which crystalline TiO_2 layers were created at RT [3-5]. We did not manage to create the crystalline layers at the mentioned conditions. After that we studied the TiO_2 fabrication on a wider deposition scale.

The layers deposited on Si(111) contained a higher amount of crystalline phase than those created at the same conditions on FS. XRD showed that most of the samples deposited according to conditions in Fig. 1 and Fig. 2 consisted of amorphous phase, but some layers exhibited polycrystalline phases of anatase (peak (103), rutile target, 6 J/cm^2, 1 Pa O_2) and rutile (peak (110), titanium target, 4 J/cm^2, 3 and 10 Pa O_2, Fig. 3). Generally rutile was found with (110) orientation, brookite with (120), (022) and anatase with (101), (103). The highest content of crystalline phase (70-90% of brookite with (120) orientation) exhibited samples annealed by RTA. All higher mentioned conditions are at T_S=200°C. There was

no observable dependence of the development of brookite phase on annealing conditions.

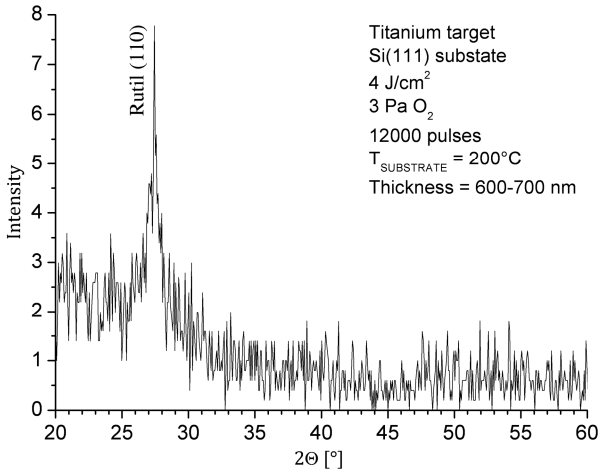

Fig. 3. XRD spectrum of TiO_2 layer containing 10-50% of rutile phase.

RS confirmed the results from XRD and even revealed some phases not measured by XRD.

In Fig. 4 we see bands near 240, 440 and 610 cm^{-1}, which confirm the presence of rutile [16]. The larger crystalline content was observed in layers prepared on oriented silicon wafers (111) (compared to those on fused silica).

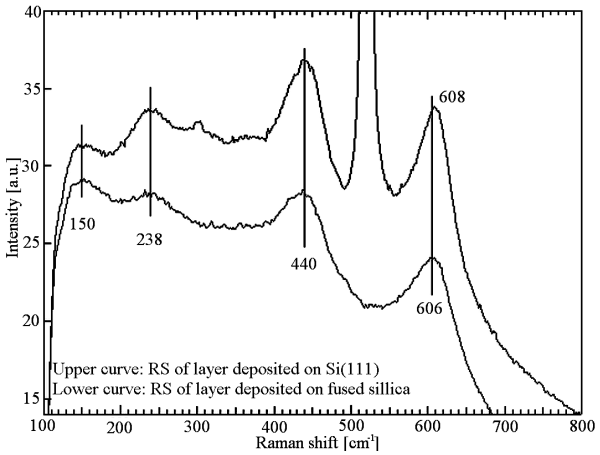

Fig. 4. Raman spectra of same sample as in Fig. 3.

The thickness of TiO_2 layers was between 0.1 and 10 μm depending on the background pressure and number of laser pulses.

Using AFM scans, we observed that the number of droplets increased with increasing fluency, especially when depositing from the titanium target. The droplet diameters ranged from 1.5 μm (4 J/cm^2) to 10 □m (9 J/cm^2). Cylindrical shape structures (Fig. 5) with dimensions from 10 to 200 nm were often combined into aggregates with a few micrometers in length. We observed those structures at RT, but they were seen more often at higher temperatures.

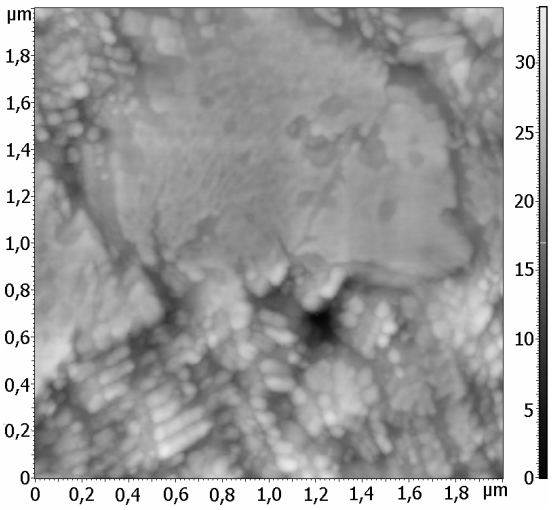

Fig. 5. AFM measurement of TiO_2 layer with anatase and brookite crystalline phase (rutile target, 4 J/cm^2, 3 Pa O_2, 300°C).

The results of the measurements concerning the photocatalytic properties of amorphous, of brookite, of rutile/brookite, and of rutile, and of anatase phases are summarized in Table 1. The best results were reached on the reference sample, which was created from 100% anatase powder (P-25, company Degussa) by a sol-gel method with crystallization at 400°C. The reference sample area was 25% larger than our samples. This can be the reason, why the results obtained from the reference sample exhibits better photocatalytic properties compared to the PLD samples.

Table 1. The photocatalytic measurement results. "Δ80 min" expresses measured pH change after 80 minutes. "Δ80 min [%]" is related to pH value at the beginning of measurement.

	TiO_2 layers prepared by PLD					Ref.
XRD phase	Amorphous	Brookite	Rutile/Brookite	Rutile	Anatase	Anatase
Δ 80 min [pH]	0,11 ÷ 0,20	0,09 ÷ 0,11	0,1 ÷ 0,21	0,30	0,17 ÷ 0,31	0,54
Δ 80 min [%]	1,80 ÷ 3,29	1,4 ÷ 2,15	1,82 ÷ 4,08	5,29	2,74 ÷ 5,06	9,57

From the measurements follows that it is difficult to tell, which crystalline phase (anatase, rutile, brookite) is better because of the unknown precise composition of phases in samples. On average, the order from the highest to the lowest photocatalytic effect follows: anatase, rutile, rutile/brookite, brookite, and amorphous phases.

4. Conclusions

In this contribution, we report the fabrication of crystalline TiO_2 layers at room or low substrate temperatures using the PLD method. We repeated without success experiments, which claimed the creation of

crystalline TiO_2 at room temperature [3-5]. Using PLD we managed to fabricate polycrystalline rutile, rutile/anatase, and anatase layers at T_S = 200°C. Using RTA we created polycrystalline brookite layers at room temperature. The surface topology of TiO_2 layers changed with the energy density and target used. The photocatalytic properties test by the measurement of pH change show that the highest photocatalytic effect was reached for rutile and anatase layers, but brookite and amorphous layers were also photocatalytically active.

Acknowledgements

This work was supported by 7. Framework programme SAFECATHETER Project CF-CP-222164. We also thank to grant MSM 6840770012 of Ministry of Education, Youth and Sport of the Czech Republic and Institutional Research Plan AVOZ 10100522.

References

[1] N. E. Stankova, I. G. Dimitrov, T. R. Stoyanchov, P. A. Atanasov, D. Kovacheva, Applied Surface Science **255,** 5275 (2009).
[2] H. Lin, A. K. Rumaiz, M. Schulz, D. Wang, R. Rock, C. P. Huang, S. I. Shah, Materials Science and Engineering B **151,** 133 (2008).
[3] X. Liu, J. Yin, Z. G. Liu, X. B. Yin, G. X. Chen, M. Wang, Applied surface science **174**, 35 (2001).
[4] M. Fusi, V. Russo, C. S. Casari, A. L Bassi, C. E. Bottani, Applied surface science **255**(10), 5334 (2009).
[5] N. Koshizaki, A. Narazaki, T. Sasaki, Applied surface science **197-198**, 624 (2002).
[6] J. M. Bennett, E. Pelletier, G. Albrand, J. P. Borgogno, B. Lazarides, Ch. K. Carniglia, R. A. Schmell, T. H. Allen, T. Tuttle-Hart, K. H. Guenther, A. Saxer, Applied Optics **28**(16), 3303 (1989).
[7] A. Kobayashi, W. Jiang, Vacuum **83,** 86 (2009).
[8] Y. W. Sakai, K. Obata, K. Hashimoto, H. Irie, Vacuum **83,** 683 (2009).
[9] N. Wang, X. Li, Y. Wang, Y. Hou, X. Zou, G. Chen, Materials Letters **62,** 3691 (2008).
[10] A. K. Sharma, R. K. Thareja, U. Willer, W. Schade, Applied surface science **206,** 137 (2003).
[11] J. M. Lackner, W. Waldhauser, R. Ebner, B. Major, T. Schöberl, Applied surface science **180-181**, 585 (2004).
[12] N. S. Allen, M. Edge, J. Verran, J. Stratton, J. Maltby, C. Bygott, Polymer Degradation and Stability **93**(9), 1632 (2008).
[13] M. F. Brunella, M. V. Diamanti, M. P. Pedeferri, F. Di Fonzo, C. S. Casari, A. Li Bassi, Thin Solid Films **515** (16), 6309 (2007).
[14] Y. Cheng, H. Sun, W. Jin, N. Xu, Chemical Engineering Journal **128,** 127 (2007).
[15] X-H. Ou, Ch-H. Wu, S-L. Lo, React. Kinet. Catal. Lett. **88,** 89 (2006).
[16] Y-H. Zhang, Ch.K. Chan, J.F. Porter, W. Guo, J. Mat. Res. **13,** 2602 (1998).

*Corresponding author:jremsa@gmail.com